

Hybrid Sparse/Diffuse Channels: a New Model and Estimators for Wideband Channels

Nicolò Michelusi*, Urbashi Mitra†, Andreas F. Molisch†, Michele Zorzi*

*Department of Information Engineering, University of Padova, Italy, {michelusi, zorzi}@dei.unipd.it

†University of Southern California, USA, {ubli, molisch}@usc.edu

Abstract—While purely sparse channel models have been recently investigated for underwater acoustic channels, experimental propagation data suggests that the channel is more complex. Thus, herein we propose a novel channel model based on both diffuse and sparse components. Tailored to this hybrid model, channel estimators are designed for different scenarios which differ in the amount of side information available at the receiver. The proposed channel estimation methods are compared to unstructured and purely sparse estimators. The numerical results show that the new channel estimation schemes considerably improve the estimation accuracy and the bit error rate performance over conventional channel estimators. Further, a mean squared error analysis of the proposed estimators is conducted in two asymptotic regimes (high SNR and low SNR) enabling a simple characterization and thus comparison of the proposed estimators.

Index Terms—Ultra Wideband, channel estimation, sparse approximations, Bayesian estimation, channel modeling

I. INTRODUCTION

UnderWater Acoustic (UWA) communication is an emerging technology, based on the transmission of sound waves, designed for applications such as environmental monitoring, marine surveillance and ocean exploration [1], [2].

The performance of coherent UWA transceivers relies on the availability of accurate channel estimation. Failure to do so results in a Bit Error Rate (BER) degradation, thus negatively affecting the upper layers of the protocol stack. For this reason, it is important to design accurate channel estimation strategies, by leveraging the statistical and structural properties of the UWA propagation channel.

Owing to the wideband nature of the UWA channel and the use of acoustic waves, which are better suited to underwater communications than conventional radio technologies, the UWA channel is characterized by large propagation delays, significant delay spread of the channel, high attenuation, low transmission bandwidth and Doppler spread [3], [4]. In particular, the low speed of sound in the water, compared to the speed of light of the radio signal, incurs large inter-arrival times of the Multi-Path Components (MPCs) relative to the delay resolution at the receiver. Hence, most MPCs, arising from scattering and reflections in the environment, can be resolved at the receiver and, in the discrete baseband representation of the channel, only some of the resolvable delay bins carry a significant energy contribution, yielding a *sparse* channel representation. For this reason, channel estimation techniques based on *sparse approximation* and *compressed*

sensing have been proposed in the literature (*e.g.*, see [5]–[8]). These techniques have been shown to outperform unstructured estimators [6]. Moreover, sparse estimators have been shown to be robust even when the channel does not exhibit a fully sparse nature [9].

However, recent propagation studies suggest that, in some scenarios of interest for UWA applications, *e.g.*, shallow water, where the reflections of the sound waves from the seabed and sea surface give rise to a richer interaction among the MPCs, also *diffuse* components are present [10]. These arise from propagation phenomena such as scattering from rough surfaces, unresolvable MPCs, inhomogeneities in the water column, causing constructive and destructive multi-path interference patterns at the receiver. These phenomena are not properly modeled by a purely sparse channel, but rather by a diffuse contribution.

To this end, in this work we propose a novel *Hybrid Sparse/Diffuse* (HSD) model for UWA channels, which is suitable for the design of channel estimation strategies and estimator analysis. The HSD model has been originally proposed in our previous work [11] for the Ultra WideBand (UWB) channel. In fact, due to their wideband nature (*i.e.*, the use of a large transmission bandwidth, relative to the carrier frequency), the UWB and UWA channels exhibit common features, *e.g.*, resolvable MPCs, diffuse scattering and frequency dispersion.

While effectively modeling the main propagation mechanisms in UWA, *e.g.*, a sparse component to model the resolvable MPCs, and a diffuse component to model diffuse scattering, unresolvable MPCs and frequency dispersion, this model can be used as a basis for the design of channel estimation strategies. Based on the HSD model, in this work we propose channel estimators for four physically motivated estimation scenarios, differing in the amount of side information available at the receiver. We compare the proposed estimators to unstructured estimators, *e.g.*, Least Squares (LS), and conventional sparse or diffuse estimators, which discard either the diffuse or the sparse component of the channel, showing that the proposed HSD model and channel estimators significantly improve the performance, from both a Mean Squared Error (MSE) and BER perspective.

Additionally, we present an high and low Signal to Noise Ratio (SNR) analysis of the MSE of the *Generalized MMSE* (G-MMSE) and *Generalized Thresholding* (G-Thres) estimators, which are designed for the case where the sparse coef-

ficients are treated as deterministic unknown parameters. We prove that in these regimes, it is beneficial to underestimate the sparsity level in the estimation of the sparse component of the channel. This behavior is confirmed by simulation and, to some extent, it holds also in the medium SNR regime where, in fact, a too aggressive approach in the estimation of the sparse component may lead to poor performance.

The paper is organized as follows. In Section II, we present the HSD model. In Section III, we discuss four estimation scenarios, which differ in the amount of side information available at the receiver for the purpose of channel estimation. In Section IV, for each scenario, we design channel estimators based on the HSD model. In Section V, we present the MSE analysis of the G-MMSE and G-Thres estimators, in the high and low SNR regimes. In Section VI, we discuss the scenario with non-orthogonal pilot sequences. In Section VII, we present simulation results. In Section VIII, we conclude the paper.

We use lower-case bold letters for column vectors (\mathbf{a}), and upper-case bold letters for matrices (\mathbf{A}). The scalar \mathbf{a}_k (or $\mathbf{a}(k)$) denotes the k th entry of vector \mathbf{a} , and $\mathbf{A}_{k,j}$ (or $\mathbf{A}(k,j)$) denotes the (k,j) th entry of matrix \mathbf{A} . The transpose, complex conjugate of \mathbf{A} is denoted by \mathbf{A}^* . A positive definite (positive semi-definite) matrix \mathbf{A} is denoted by $\mathbf{A} \succ 0$ ($\mathbf{A} \succeq 0$). The $K \times K$ identity matrix is defined as \mathbf{I}_K . The vector $\mathbf{a} \odot \mathbf{b}$ is the component-wise (Schur) product of vectors \mathbf{a} and \mathbf{b} . We use $p(\cdot)$ to indicate a continuous or discrete probability distribution, and $\Pr(\cdot)$ to indicate the probability of an event. The expectation of random variable x , conditioned on y , is given by $\mathbb{E}[x|y]$. The circularly symmetric complex Gaussian distribution with mean \mathbf{m} and covariance matrix $\mathbf{\Sigma}$ is denoted by $\mathcal{CN}(\mathbf{m}, \mathbf{\Sigma})$; the Bernoulli distribution with parameter q is denoted by $\mathcal{B}(q)$.

II. SYSTEM MODEL

A. Observation Model

We consider a single-user system. The source transmits an orthogonal pilot sequence $x(n), n = -L + 1, \dots, N - 1$. At the receiver, we have

$$y(k) = \sum_{l=0}^{L-1} h(l)x(k-l) + w(k), \quad k = 0, \dots, N-1, \quad (1)$$

where $h(l), l = 0, \dots, L-1$ is the discrete baseband representation of the channel, with delay spread $L \geq 1$, $N \geq L$ is the length of the observed sequence, and $w(k) \sim \mathcal{CN}(0, \sigma_w^2), k = 0, \dots, N-1$ is an i.i.d. noise sequence.

We can restate the observation model in matrix form as

$$\mathbf{y} = \mathbf{X}\mathbf{h} + \mathbf{w}, \quad (2)$$

where $\mathbf{X} \in \mathbb{C}^{N \times L}$ is the Toeplitz matrix associated with the pilot sequence, $\mathbf{h} = [h(0), h(1), \dots, h(L-1)]^T$ is the channel vector, and $\mathbf{w} = [w(0), w(1), \dots, w(N-1)]^T \sim \mathcal{CN}(\mathbf{0}, \sigma_w^2 \mathbf{I}_L)$ is the noise vector.

Since the Least Squares (LS) estimate is a sufficient statistic for estimating the channel, we employ the following observation model, rather than (2):

$$\mathbf{h}_{LS} = (\mathbf{X}^* \mathbf{X})^{-1} \mathbf{X}^* \mathbf{y} = \mathbf{h} + \sqrt{S}^{-1} \mathbf{n}, \quad (3)$$

where, due to the orthogonality of the pilot sequence, we have assumed $\sigma_w^{-2} \mathbf{X}^* \mathbf{X} = S \mathbf{I}_L$, and $\mathbf{n} \sim \mathcal{CN}(\mathbf{0}, \mathbf{I}_L)$ is the noise vector; we define $S > 0$ to be the estimation SNR. In the following, with a slight abuse of notation, we refer to \mathbf{h}_{LS} as the *observed sequence*, and to $\sqrt{S}^{-1} \mathbf{n}$ as the *noise sequence*.

B. Channel Model

The channel \mathbf{h} obeys the HSD model [11]–[13]

$$\mathbf{h} = \mathbf{h}_s + \mathbf{h}_d, \quad (4)$$

where $\mathbf{h}_s = \mathbf{a}_s \odot \mathbf{c}_s$ is the *sparse component*, and \mathbf{h}_d is the *diffuse* one. In particular, the vector \mathbf{a}_s is the *sparsity pattern*, with Bernoulli entries with $\Pr(\mathbf{a}_s(k) = 1) = q \quad \forall k$, where q represents the *sparsity level* of the channel. The vector \mathbf{c}_s is the *sparse coefficients vector*. Notice that this is a *dense* vector; however, the sparsity pattern \mathbf{a}_s , which is expected to exhibit few non-zero entries, owing to its Bernoulli nature, selects the active entries from the sparse coefficient vector, so that \mathbf{h}_s is sparse. We assume $\mathbb{E}[\mathbf{c}_s \mathbf{c}_s^*] = \mathbf{\Lambda}_s$, where $\mathbf{\Lambda}_s$ is diagonal with entries given by the PDP of the active sparse components $\mathbf{\Lambda}_s(k, k) = \mathcal{P}_s(k), k = 0, \dots, L-1$. Finally, the diffuse component obeys $\mathbf{h}_d \sim \mathcal{CN}(\mathbf{0}, \mathbf{\Lambda}_d)$, where the covariance matrix $\mathbf{\Lambda}_d$ is diagonal with entries given by the PDP $\mathbf{\Lambda}_d(k, k) = \mathcal{P}_d(k), k = 0, \dots, L-1$.

III. CHANNEL ESTIMATION SCENARIOS

The HSD model introduced in Section II-B is parameterized by the sparsity level q , the PDP of the diffuse component $\mathcal{P}_d(\cdot)$, and the PDP of the sparse component $\mathcal{P}_s(\cdot)$. These parameters are not available at the receiver *a priori*, but need to be estimated. The ability of the receiver to estimate them depends on a number of factors, including the length of the observation window available at the receiver for channel estimation purposes and the degree of mobility.

Notice that the sparse component \mathbf{h}_s arises from resolvable MPCs due to reflections and scattering in the surrounding environment. Significant variations of the amplitude and delays of these components happen on a relatively large time-scale (large scale fading), due to the relative motion of the transmitter, receiver and scatterers. Hence, the PDP $\mathcal{P}_s(\cdot)$ can be estimated over a "large" observation window, sufficient to average over the large scale fading.

On the other hand, the diffuse component \mathbf{h}_d arises from propagation phenomena such as the unresolvable MPCs or scattering from rough surfaces. Significant variations of the diffuse component happen on a much shorter time-scale (small scale fading). Hence, the PDP $\mathcal{P}_d(\cdot)$ can be accurately estimated over a "short" observation window, sufficient to average over the small scale fading.

Alternatively, we can exploit the structure of the PDP $\mathcal{P}_d(\cdot)$ to average the fading over the delay dimension, rather

than over subsequent realizations of the fading process. In particular, we assume an exponential PDP $\mathcal{P}_d(k) = \beta e^{-\omega k}$, parameterized by the power β and the decay rate ω . We can exploit this low order parameterization of the PDP to enhance the estimation accuracy. In the limit, with this approach we can estimate the PDP based on a single snapshot of the channel.

As to the sparsity level q , it can be estimated by first separating the diffuse and sparse components, and then by counting the occurrences of active sparse components. In order to separate the sparse component from the diffuse one, we need at least an estimate of the PDP $\mathcal{P}_d(\cdot)$. Hence, we assume that the sparsity level q can be estimated over an observation window larger than the one required to estimate the PDP $\mathcal{P}_d(\cdot)$, but shorter than the one required to estimate the PDP $\mathcal{P}_s(\cdot)$.

Based on these considerations, depending on the length of the observation window available at the receiver, we identify four different scenarios listed in Table I, differing in the amount of side information which can be exploited at the receiver in the estimation phase.

In the next section, we design channel estimators for each estimation scenario.

TABLE I

ESTIMATION SCENARIOS, BASED ON THE AMOUNT OF SIDE INFORMATION AVAILABLE AT THE RECEIVER. K: KNOWN, U: UNKNOWN.

	Scenario	Λ_d	q	Λ_s	Estimator
S1	Single Snapshot of the channel	U	U	U	LS
S2	Single Snapshot of the channel (PDP structure exploited)	K	U	U	G-MMSE, G-Thres
S3	Avg. over Small scale fading	K	K	U	G-MMSE, G-Thres
S4	Avg. over Small & Large scale fading	K	K	K	MMSE

IV. CHANNEL ESTIMATORS FOR THE HSD MODEL

In this Section, we design estimators for scenarios S2, S3 and S4 in Table I. Scenario S1 will not be further considered, since in this case we use the LS estimator \mathbf{h}_{LS} . In particular, in Section IV-A we design the G-MMSE and G-Thres estimators for scenarios S2 and S3. In Section IV-B, we design the MMSE estimator for scenario S4.

A. G-MMSE and G-Thres estimators (Scenarios S2 and S3)

For these scenarios, we assume that the PDP $\mathcal{P}_d(\cdot)$ is known at the receiver, whereas the PDP $\mathcal{P}_s(\cdot)$ is unknown, so that \mathbf{c}_s is treated as a deterministic unknown vector.

We also assume that the sparsity level q is unknown (this is true in scenario S2, but false in scenario S3), and an estimate \tilde{q} of q , which might be different from the real q , is used in the estimation phase. This approach differs from [11], where the true sparsity level is used. In Section V, and by simulation in Section VII, we will show that using $\tilde{q} < q$ often improves the MSE estimation accuracy, thus implying that exact knowledge of this parameter is not crucial to the performance of the estimators.

The G-MMSE and G-Thres estimators are given by the following steps:

- 1) The sparse coefficient vector \mathbf{c}_s (modeled as a deterministic unknown vector) is estimated via Maximum Likelihood (ML), assuming \mathbf{h}_d as noise. We have $\hat{\mathbf{c}}_s = \mathbf{h}_{LS}$.
- 2) The sparsity pattern is estimated via either MMSE (G-MMSE estimator) or MAP (G-Thres estimator), assuming \mathbf{h}_d as noise, $\hat{\mathbf{c}}_s = \mathbf{h}_{LS}$, and the sparsity level \tilde{q} , rather than the true q . We have

$$\hat{\mathbf{a}}_s(k) = \begin{cases} \frac{1}{1 + e^\alpha \exp\left\{-\frac{S|\mathbf{h}_{LS}(k)|^2}{1 + S\mathcal{P}_d(k)}\right\}} & \text{MMSE} \\ \mathcal{I}\left(|\mathbf{h}_{LS}(k)|^2 \geq \alpha \frac{1 + S\mathcal{P}_d(k)}{S}\right) & \text{MAP,} \end{cases} \quad (5)$$

where $\mathcal{I}(\cdot)$ is the indicator function, and we have defined $\alpha = \ln\left(\frac{1 - \tilde{q}}{\tilde{q}}\right)$.

- 3) The sparse component is estimated as

$$\hat{\mathbf{h}}_s = \hat{\mathbf{a}}_s \odot \hat{\mathbf{c}}_s = \hat{\mathbf{a}}_s \odot \mathbf{h}_{LS}. \quad (6)$$

- 4) The diffuse component is estimated by MMSE, based on the residual estimation error $\mathbf{h}_{LS} - \hat{\mathbf{h}}_s$:

$$\hat{\mathbf{h}}_d(k) = \frac{S\mathcal{P}_d(k)}{1 + S\mathcal{P}_d(k)}(1 - \hat{\mathbf{a}}_s(k))\mathbf{h}_{LS}(k), \quad \forall k. \quad (7)$$

- 5) The overall HSD estimate is given by

$$\hat{\mathbf{h}} = \hat{\mathbf{h}}_s + \hat{\mathbf{h}}_d. \quad (8)$$

B. MMSE estimator (Scenario S4)

In scenario S4, the receiver knows all the deterministic parameters of the channel, *i.e.*, the PDPs of the sparse and diffuse components, $\mathcal{P}_s(\cdot)$ and $\mathcal{P}_d(\cdot)$, respectively, and the sparsity level q . Under this assumption, we can design an MMSE estimator of the channel, which clearly minimizes the MSE. We assume $\mathbf{c}_s \sim \mathcal{CN}(\mathbf{0}, \Lambda_s)$, which leads to the classical Gaussian (linear) MMSE estimator of the sparse coefficient vector.

The MMSE estimator develops along the following steps, for all $k = 0, \dots, L - 1$:

- 1) Assuming $\mathbf{a}_s(k) = 0$ (no active sparse component), perform an MMSE estimate of the diffuse component:

$$\mathbf{h}_d^{(MMSE)}(k) = \frac{S\mathcal{P}_d(k)}{1 + S\mathcal{P}_d(k)}\mathbf{h}_{LS}(k). \quad (9)$$

- 2) Assuming $\mathbf{a}_s(k) = 1$ (the k th channel entry is the sum of sparse and diffuse components), perform a linear MMSE estimate of the sparse+diffuse channel entry:

$$\mathbf{h}_{s+d}^{(MMSE)}(k) = \frac{S(\mathcal{P}_s(k) + \mathcal{P}_d(k))}{1 + S(\mathcal{P}_s(k) + \mathcal{P}_d(k))}\mathbf{h}_{LS}(k). \quad (10)$$

- 3) The overall estimate is the weighted sum of $\mathbf{h}_{s+d}^{(MMSE)}(k)$ and $\mathbf{h}_d^{(MMSE)}(k)$, weighted by the posterior probability of an active and non-active sparse component, respectively. This is given by

$$\begin{aligned} \hat{\mathbf{h}}_{MMSE}(k) &= \mathbb{E}[\mathbf{h}(k) | \mathbf{h}_{LS}(k)] \\ &= q_{post}(k)\mathbf{h}_{s+d}^{(MMSE)}(k) + (1 - q_{post}(k))\mathbf{h}_d^{(MMSE)}(k), \end{aligned} \quad (11)$$

where, using Bayes' theorem and letting $\rho_k = \frac{S\mathcal{P}_s(k)}{1+S\mathcal{P}_d(k)}$, we have defined

$$q_{post}(k) = \Pr(\mathbf{a}_s(k) = 1 | \mathbf{h}_{LS}(k)) \quad (12)$$

$$= \frac{1}{1 + \frac{1-q}{q} (1 + \rho_k) \exp\left\{-\rho_k \frac{S|\mathbf{h}_{LS}(k)|^2}{1+S(\mathcal{P}_s(k)+\mathcal{P}_d(k))}\right\}}.$$

V. MSE ANALYSIS

In this section, we perform the MSE analysis of the G-MMSE and G-Thres estimators, which allows a concise performance comparison of the two estimators.

We define the MSE of the estimator $\hat{\mathbf{h}}$ as a function of the estimation SNR S as

$$MSE(S) = \mathbb{E} \left[\left\| \hat{\mathbf{h}} - \mathbf{h} \right\|_2^2 \right] = \sum_{k=0}^{L-1} \mathbb{E} \left[\left| \hat{\mathbf{h}}(k) - \mathbf{h}(k) \right|^2 \right]. \quad (13)$$

The expectation is computed with respect to the realizations of the channel \mathbf{h} and of the noise \mathbf{n} (the estimator is a deterministic function of $\mathbf{h}_{LS} = \mathbf{h} + \sqrt{S}^{-1}\mathbf{n}$).

Due to the difficulty in studying the MSE performance in the medium SNR range, we perform the analysis in the low and high SNR regimes. Moreover, as a consequence of the decomposition (13), and since we are considering per-tap estimation approaches (which are optimal under our assumption of orthogonal pilot sequences), it is sufficient to study the asymptotic behavior of the MSE associated with the estimator of the k th channel tap, *i.e.*,

$$MSE_k(S) = \mathbb{E} \left[\left| \hat{\mathbf{h}}(k) - \mathbf{h}(k) \right|^2 \right]. \quad (14)$$

For ease of notation, we define $y = \mathbf{h}_{LS}(k)$, $\hat{h}(y) = \hat{\mathbf{h}}(k)$, $a_s = \mathbf{a}_s(k) \sim \mathcal{B}(q)$, $c_s = \mathbf{c}_s(k)$, $h_d = \frac{1}{\sqrt{\mathcal{P}_d(k)}}\mathbf{h}_d(k) \sim \mathcal{CN}(0,1)$ (normalized to the power of the diffuse component), $h = \mathbf{h}(k)$, $n = \mathbf{n}(k) \sim \mathcal{CN}(0,1)$, $P_d = \mathcal{P}_d(k)$ and $MSE(S) = MSE_k(S) = \mathbb{E} \left[\left| \hat{h}(y) - h \right|^2 \right]$. Moreover, we define $f(\sqrt{S}y, n) = S \left| \hat{h}(y) - h \right|^2$, so that $MSE(S) = \frac{1}{S} \mathbb{E} \left[f(\sqrt{S}h + n, n) \right]$. We use the proper sub-script to distinguish between different estimators, when necessary. With this notation, the observation model associated with the k th channel entry is given by

$$y = a_s c_s + \sqrt{P_d} h_d + \frac{1}{\sqrt{S}} n. \quad (15)$$

Notice that for the LS estimator $\hat{h}(y) = y$ we have $MSE_{LS}(S) = S^{-1}$. Alternatively, $S \cdot MSE_{LS}(S) = 1, \forall S > 0$. Similarly, for the G-MMSE and G-Thres estimators, in the high and low SNR we have, for $S_{lim} \in \{0, +\infty\}$,

$$\lim_{S \rightarrow S_{lim}} S \cdot MSE(S) = \lim_{S \rightarrow S_{lim}} \mathbb{E} \left[f(\sqrt{S}h + n, n) \right] = Q_{S_{lim}}.$$

We study the asymptotic behavior $Q_{S_{lim}}$ of the G-MMSE and G-Thres estimators in the following regions:

- High SNR, no diffuse component ($S_{lim} = +\infty$, $\mathcal{P}_d(k) = 0 \quad \forall k$)

- High SNR, with diffuse component ($S_{lim} = +\infty$, $\mathcal{P}_d(k) > 0 \quad \forall k$)
- Low SNR ($S_{lim} = 0$).

We have the following Lemma. Due to space limitations, the proof is given in [13].

Lemma 1 (Exchange of limit and expectation). For the G-MMSE and G-Thres estimators, $S_{lim} \in \{0, +\infty\}$, we have

$$\lim_{S \rightarrow S_{lim}} S \cdot MSE(S) = \mathbb{E} \left[\lim_{S \rightarrow S_{lim}} f(\sqrt{S}h + n, n) \right].$$

A. High SNR, no diffuse component

In the high SNR region ($S \rightarrow +\infty$) with $P_d = 0$, for the G-MMSE estimator we have

$$\lim_{S \rightarrow +\infty} f_{G-MMSE}(\sqrt{S}a_s c_s + n, n) \quad (16)$$

$$= \begin{cases} \left| \frac{n}{1 + e^\alpha \exp\{-|n|^2\}} \right|^2, & a_s = 0 \\ |n|^2, & a_s = 1. \end{cases}$$

Taking the expectation, by averaging over $a_s \sim \mathcal{B}(q)$, $n \sim \mathcal{CN}(0,1)$, and using Lemma 1, we obtain

$$\lim_{S \rightarrow +\infty} S \cdot MSE_{G-MMSE}(S) = q + (1-q)g(\tilde{q}), \quad (17)$$

where we have defined

$$g(\tilde{q}) = \mathbb{E} \left[\left| \frac{n}{1 + e^\alpha \exp\{-|n|^2\}} \right|^2 \right] = -\frac{\tilde{q}}{1-\tilde{q}} \ln \tilde{q}. \quad (18)$$

Similarly, for the G-Thres estimator, in the high SNR region ($S \rightarrow +\infty$) we have

$$\lim_{S \rightarrow +\infty} f_{G-Thres}(\sqrt{S}a_s c_s + n, n) \quad (19)$$

$$= \begin{cases} |n|^2 & a_s = 1 \\ \mathcal{I}(|n|^2 \geq \alpha) |n|^2, & a_s = 0. \end{cases}$$

Taking the expectation, by averaging over $a_s \sim \mathcal{B}(q)$, $n \sim \mathcal{CN}(0,1)$, using Lemma 1 we obtain

$$\lim_{S \rightarrow +\infty} S \cdot MSE_{G-Thres}(S) = q + (1-q)w(\tilde{q}), \quad (20)$$

where we have defined

$$w(\tilde{q}) = \begin{cases} \frac{\tilde{q}}{1-\tilde{q}} \left(1 + \ln \frac{1-\tilde{q}}{\tilde{q}} \right) & \tilde{q} < \frac{1}{2} \\ 1 & \tilde{q} \geq \frac{1}{2}. \end{cases} \quad (21)$$

This result can be interpreted as follows. When $\mathbf{a}_s(k) = 1$ (with probability q), the active sparse component is detected with no error, since the sparse coefficient can be clearly distinguished from the noise, and the sparse coefficient is estimated with the same accuracy as LS. When $\mathbf{a}_s(k) = 0$ (with probability $1-q$), a mis-detection error $MSE_{LS}(S)g(\tilde{q})$ or $MSE_{LS}(S)w(\tilde{q})$ (in the MSE sense) is incurred due to strong noise peaks, which may be mis-detected as active sparse components.

B. High SNR, with diffuse component

When $P_d > 0$, in the high SNR region, for both the G-MMSE and G-Thres estimators we obtain

$$\begin{aligned} & \lim_{S \rightarrow +\infty} f_{G-MMSE}(\sqrt{S}h + n, n) \\ &= \lim_{S \rightarrow +\infty} f_{G-Thres}(\sqrt{S}h + n, n) = |n|^2. \end{aligned} \quad (22)$$

From Lemma 1, the high SNR MSE asymptotic behavior is given by

$$\begin{aligned} & \lim_{S \rightarrow +\infty} S \cdot MSE_{G-MMSE}(S) \\ &= \lim_{S \rightarrow +\infty} S \cdot MSE_{G-Thres}(S) = \mathbb{E}[|n|^2] = 1. \end{aligned} \quad (23)$$

Therefore, the G-MMSE and G-Thres estimators achieve the same accuracy as LS in the high SNR with diffuse component. This result is a consequence of the fact that, in the high SNR, the HSD channel is much stronger than the noise, and the overall channel exhibits a *dense* structure, hence an unconstrained estimator achieves the best estimation accuracy.

C. Low SNR

In the low SNR, we have

$$\begin{cases} \lim_{S \rightarrow 0} f_{G-MMSE}(\sqrt{S}h + n, n) = \left| \frac{n}{1 + e^\alpha \exp\{-|n|^2\}} \right|^2 \\ \lim_{S \rightarrow 0} f_{G-Thres}(\sqrt{S}h + n, n) = \mathcal{I}(|n|^2 \geq \alpha) |n|^2. \end{cases}$$

From Lemma 1, we finally obtain the following low SNR asymptotic behavior of the MSE

$$\begin{cases} \lim_{S \rightarrow 0} S \cdot MSE_{G-MMSE}(S) = g(\tilde{q}) \\ \lim_{S \rightarrow 0} S \cdot MSE_{G-Thres}(S) = w(\tilde{q}), \end{cases} \quad (24)$$

where functions $g(\tilde{q})$ and $w(\tilde{q})$ are defined in (18) and (21), respectively.

D. Summary

The asymptotic MSE behavior of the G-MMSE and G-Thres estimators is summarized in Table II, and plotted in Figure 1.

In particular, we compare their limiting behavior with the LS estimator, and with an oracle estimator, which assumes perfect knowledge of the sparsity pattern \mathbf{a}_s and hence performs a LS estimate of the active sparse components $\mathbf{a}_s \odot \mathbf{c}_s$, and a MMSE estimate of \mathbf{h}_d . By averaging over the channel

TABLE II
ASYMPTOTIC MSE BEHAVIOR OF LS, ORACLE, G-MMSE AND G-THRES ESTIMATORS

$\frac{MSE(S)}{MSE_{LS}(S)}$	High SNR, $\Lambda_d = 0$	High SNR, $\Lambda_d > 0$	Low SNR
LS	1	1	1
Oracle	q	1	q
G-MMSE	$q + (1-q)g(\tilde{q})$	1	$g(\tilde{q})$
G-Thres	$q + (1-q)w(\tilde{q})$	1	$w(\tilde{q})$

realizations of the HSD model, its MSE as a function of the SNR S is given by

$$MSE_{Oracle}(S) = q \frac{L}{S} + (1-q) \sum_{k=0}^{L-1} \frac{\mathcal{P}_d(k)}{1 + S\mathcal{P}_d(k)}. \quad (25)$$

Notice that $g(\tilde{q})$ and $w(\tilde{q})$ are increasing functions of \tilde{q} , with $g(\tilde{q}) \leq 1$, $w(\tilde{q}) \leq 1$, $\lim_{\tilde{q} \rightarrow 1} g(\tilde{q}) = \lim_{\tilde{q} \rightarrow 1} w(\tilde{q}) = 1$, $\lim_{\tilde{q} \rightarrow 0} g(\tilde{q}) = \lim_{\tilde{q} \rightarrow 0} w(\tilde{q}) = 0$. Therefore, in the high SNR with no diffuse component and in the low SNR, the G-MMSE and G-Thres estimators perform better than the LS estimator. Moreover, the smaller \tilde{q} , the better the MSE accuracy. This proves that, from the perspective of minimizing the MSE, it is beneficial to use a conservative approach in the estimation of the sparse component. In particular, using $\tilde{q} < q$ improves the estimation accuracy with respect to using the true value of the sparsity level q .

Notice that this behavior may not hold for medium SNR, where in fact a smaller \tilde{q} may induce a larger MSE. This can be observed by studying the two extreme cases $\tilde{q} = 1$ and $\tilde{q} = 0$. When $\tilde{q} = 1$, the channel, from the perspective of the estimator, is modeled as $\mathbf{h} = \mathbf{c}_s + \mathbf{h}_d$, hence the G-MMSE and the G-Thres estimators are equivalent to LS. On the other hand, when $\tilde{q} = 0$, the channel is modeled as $\mathbf{h} = \mathbf{h}_d$, and the two estimators are equivalent to the MMSE estimator of the diffuse component, with MSE

$$\begin{aligned} MSE_{diff}(S) &= \sum_{k=0}^{L-1} \mathbb{E} \left[\left| \hat{\mathbf{h}}_{diff}(k) - \mathbf{h}(k) \right|^2 \right] \\ &= \sum_{k=0}^{L-1} \left(q \frac{\mathcal{P}_s(k)}{(1 + S\mathcal{P}_d(k))^2} + \frac{\mathcal{P}_d(k)}{1 + S\mathcal{P}_d(k)} \right). \end{aligned} \quad (26)$$

Clearly, this estimator performs worse than LS ($MSE_{diff}(S) > MSE_{LS}(S)$), for any value of the SNR S , for sufficiently large values of $\mathcal{P}_s(k)$, $k = 0, \dots, L-1$.

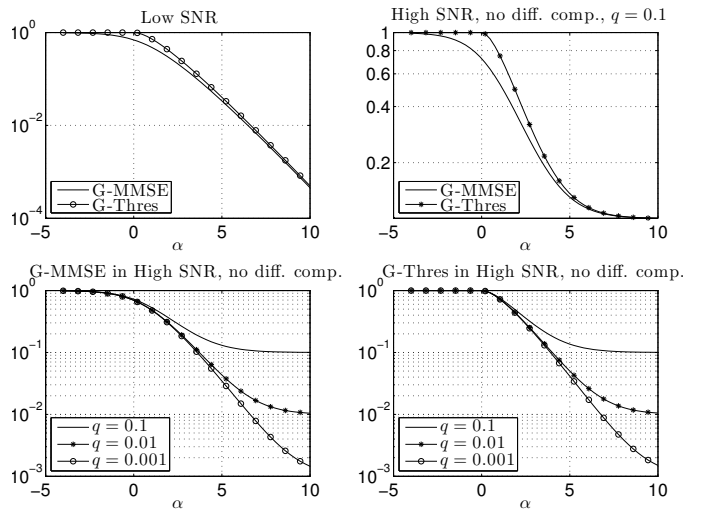


Fig. 1. High and Low asymptotic SNR behavior of $\frac{MSE(S)}{MSE_{LS}(S)}$ of the G-MMSE, G-Thres, oracle and LS estimators as a function of $\alpha = \ln \frac{1-\tilde{q}}{q}$.

Therefore, although representing the most conservative approach, the choice $\tilde{q} = 0$ may attain poor performance for medium SNR.

It is worth noticing that, while a conservative approach ($\tilde{q} < q$) is often beneficial for the G-MMSE and the G-Thres estimators, when $\mathbf{c}_s \sim \mathcal{CN}(\mathbf{0}, \mathbf{\Lambda}_s)$ the MSE of the MMSE estimator in Section IV-B is minimized by using the true sparsity level q (in fact the posterior mean minimizes the MSE). Therefore, this result can be explained with the fact that a conservative approach in the estimation of the sparse component compensates for the uncertainty on the sparse coefficient vector \mathbf{c}_s , which is treated as a deterministic and unknown vector, hence attaining a better MSE accuracy.

Finally, it can be shown that $g(\tilde{q}) \leq w(\tilde{q})$, and therefore the G-MMSE estimator outperforms the G-Thres estimator. In fact, the MMSE estimate of the sparsity pattern represents a *soft* decision of \mathbf{a}_s , and therefore expresses also the reliability associated with the detection of an active sparse component. On the other hand, the MAP estimator provides a *hard* estimate of \mathbf{a}_s , which completely discards the information about its reliability.

VI. NON-ORTHOGONAL PILOT SEQUENCES

So far, we have used the assumption of orthogonal pilot sequence. As a consequence, a per-tap estimation approach is optimal, since the entries of the noise vector $\sqrt{\mathbf{S}}^{-1} \mathbf{n}$ and of the observed sequence \mathbf{h}_{LS} are statistically independent.

Herein, we discuss the scenario where a non-orthogonal pilot sequence is employed. In this case, we have

$$\mathbf{h}_{LS} = \mathbf{h} + \sqrt{\mathbf{S}}^{-1} \mathbf{n}, \quad (27)$$

where we have defined the SNR matrix $\mathbf{S} = \frac{\mathbf{X}^* \mathbf{X}}{\sigma_w^2}$. While in the orthogonal case \mathbf{S} is diagonal, thus decoupling the entries of the observed sequence, in the non-orthogonal case it has non-zero off-diagonal components.

In this case, a per-tap estimation approach, by discarding the noise correlation structure over the channel delay dimension, is sub-optimal and incurs a performance loss, which can be characterized as an effective SNR loss (see, *e.g.*, [13]).

In order to exploit the noise correlation structure, we need to design *joint* estimation techniques. To this end, we now explore the connection between the G-Thres estimator and classical sparse approximation algorithms [14], [15].

Letting $\mathbf{h}_s = \mathbf{a}_s \odot \mathbf{c}_s$, the G-Thres estimator solves

$$\begin{aligned} \{\hat{\mathbf{c}}_s, \hat{\mathbf{a}}_s, \hat{\mathbf{h}}_d\} &= \arg \max_{\mathbf{c}_s, \mathbf{a}_s, \mathbf{h}_d} p(\mathbf{h}_{LS}, \mathbf{a}_s, \mathbf{h}_d | \mathbf{c}_s) \\ &= \arg \min_{\mathbf{h}_s = \mathbf{a}_s \odot \mathbf{c}_s, \mathbf{h}_d} (\mathbf{h}_{LS} - \mathbf{h}_s - \mathbf{h}_d)^* \mathbf{S} (\mathbf{h}_{LS} - \mathbf{h}_s - \mathbf{h}_d) \\ &\quad + \alpha \|\mathbf{h}_s\|_0 + \mathbf{h}_d^* \mathbf{\Lambda}_d^{-1} \mathbf{h}_d. \end{aligned} \quad (28)$$

This problem can be viewed as a LS regression problem, with an \mathcal{L}_0 regularization term associated with \mathbf{h}_s ($\|\mathbf{h}_s\|_0 = \sum_{k=0}^{L-1} \mathcal{I}(|\mathbf{h}_s(k)| > 0)$), enforcing sparseness of the solution, and an \mathcal{L}_2 regularization term associated with \mathbf{h}_d , enforcing the Gaussian nature of the diffuse component.

The solution of (28) with respect to \mathbf{h}_d first, as a function of \mathbf{h}_s , gives the MMSE estimator

$$\hat{\mathbf{h}}_d(\mathbf{h}_s) = \mathbf{\Lambda}_d \mathbf{\Sigma}_{d+n}^{-1} (\mathbf{h}_{LS} - \mathbf{h}_s), \quad (29)$$

where we have defined $\mathbf{\Sigma}_{d+n} = \mathbf{\Lambda}_d + \mathbf{S}^{-1}$. By substituting this solution into the cost function, we obtain

$$\hat{\mathbf{h}}_s = \arg \min_{\mathbf{h}_s \in \mathbb{C}^L} (\mathbf{h}_{LS} - \mathbf{h}_s)^* \mathbf{\Sigma}_{d+n}^{-1} (\mathbf{h}_{LS} - \mathbf{h}_s) + \alpha \|\mathbf{h}_s\|_0. \quad (30)$$

This can be viewed as a LS regression problem, with an \mathcal{L}_0 term associated with \mathbf{h}_s , where \mathbf{h}_d is treated as noise.

The optimal solution of the above problem requires a combinatorial search over all the possible realizations of the sparsity pattern \mathbf{a}_s . Otherwise, we need to recur to numerical algorithms, which have been extensively researched in the literature. An equivalent problem is addressed in [14], namely

$$\hat{\mathbf{h}}_s = \arg \min_{\mathbf{h}_s \in \mathbb{C}^L} \|\mathbf{w} - \Phi \mathbf{h}_s\|_2^2 + \lambda \|\mathbf{h}_s\|_0, \quad (31)$$

where \mathbf{w} is a noisy version of $\Phi \mathbf{h}_s$, and Φ is known, with $\mathbf{I}_L - \Phi^* \Phi \succ 0$. Equation (30) is equivalent to (31) by letting $\mathbf{w} = \sqrt{\rho} \mathbf{\Sigma}_{d+n}^{-\frac{1}{2}} \mathbf{h}_{LS}$, $\Phi = \sqrt{\rho} \mathbf{\Sigma}_{d+n}^{-\frac{1}{2}}$, and $\lambda = \rho \alpha$, where $\rho > 0$ is chosen so as to guarantee $\mathbf{I}_L - \Phi^* \Phi \succ 0$. The *Iterative Thresholding Algorithm* proposed in [14] may then be used to estimate \mathbf{h}_s , and equation (29) to estimate the diffuse component \mathbf{h}_d , after convergence of the iterative algorithm.

Alternatively, we may relax the \mathcal{L}_0 cost associated with \mathbf{h}_s , and use a \mathcal{L}_1 regularization term instead [15], thus giving

$$\hat{\mathbf{h}}_s = \arg \min_{\mathbf{h}_s \in \mathbb{C}^L} (\mathbf{h}_{LS} - \mathbf{h}_s)^* \mathbf{\Sigma}_{d+n}^{-1} (\mathbf{h}_{LS} - \mathbf{h}_s) + \alpha \|\mathbf{h}_s\|_1, \quad (32)$$

where $\|\mathbf{h}_s\|_1 = \sum_{k=0}^{L-1} |\mathbf{h}_s(k)|$.

VII. SIMULATION RESULTS

In this section, we present the simulation results, and evaluate the performance achievable with the proposed estimators, from both a MSE and a BER perspective.

In particular, for the simulations we generate the HSD channel $\mathbf{h} \in \mathbb{C}^L$ according to Section II-B, with delay spread $L = 50$, sparsity level $q = 0.1$, exponential PDP of the diffuse component $\mathcal{P}_d(k) = \beta e^{-\omega k}$, with $\beta = 0.01$, $\omega = 0.1$, and PDP of the sparse coefficients $\mathcal{P}_s(k) = e^{-\omega k}$. The sparse coefficients are drawn as $\mathbf{c}_s(k) \sim \mathcal{CN}(0, \mathcal{P}_s(k))$.

We consider the unstructured LS estimator (scenario S1 in Table I), the G-MMSE and G-Thres estimators, for different values of the assumed sparsity level $\tilde{q} \in \{0.1, 0.01, 0.001\}$ (Scenarios S2 and S3 in Table I) and the MMSE estimator (scenario S4 in Table I). The latter, by minimizing the MSE, represents a bound to the estimation accuracy, hence it is primarily used as a reference for the other estimators. Moreover, we also consider a *Sparse* estimator, which neglects the contribution from the diffuse component (in particular, we use a variation of the G-Thres estimator which assumes $\mathcal{P}_d(k) = 0, \forall k$), and a *Diffuse* estimator, which, on the other hand, neglects the sparse component (in particular, it is the limit case of the G-MMSE or G-Thres estimators with $\tilde{q} = 0$).

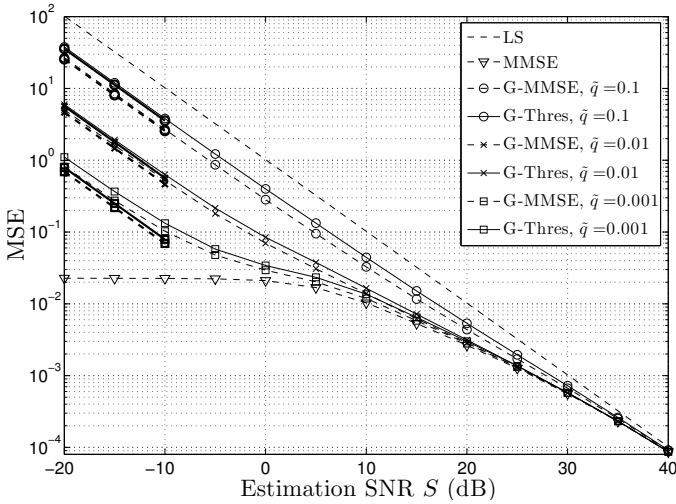


Fig. 2. MSE of the G-MMSE and G-Thres estimators. The bold lines with the corresponding markers represent the low SNR asymptotic MSE behavior. The high SNR asymptotic behavior is given by the LS estimate.

In Figure 2, we plot the MSE of the G-MMSE and G-Thres estimators as a function of the estimation SNR S , for different values of the assumed sparsity level \tilde{q} , and their asymptotic MSE behavior (bold lines, with the corresponding markers for the different values of \tilde{q}). We notice that there is a perfect match between the MSE in the high and low SNR ranges, and the asymptotic behavior developed in Section V. In particular, the results confirm that it is beneficial to use a conservative approach in the estimation of the sparse component. Also, as predicted by the MSE analysis, the G-MMSE estimator outperforms the G-Thres estimator, in the asymptotic regimes. To some extent, this behavior is observed also in the medium SNR range. However, this is not true in general: in fact, the *Diffuse* estimator in Figure 3, which is equivalent to G-MMSE/G-Thres with $\tilde{q} = 0$, represents the most conservative approach in the estimation of the sparse component; nevertheless, it performs worse than LS for medium SNR.

In Figure 3, we compare the MSE of the G-Thres, Sparse and Diffuse estimators, assuming the sparsity level $\tilde{q} = 0.001$. We notice that both the Sparse and the Diffuse estimators incur a performance loss in the medium SNR range, due to the fact that either the diffuse or the sparse component is neglected.

In Figure 4, we plot the BER induced by channel estimation errors. In particular, for the BER computation, we consider an OFDM system, employing $N_{dft} = 256$ sub-carriers and a 4-QAM constellation. Since we are interested in evaluating how estimation errors affect the BER performance, we consider a scenario where noise is added in the estimation phase, so as to induce channel estimation errors, while noise is not added to the information symbols. We notice that the G-MMSE estimator with $\tilde{q} = 0.001$ performs very closely to the lower bound, represented by the BER of the MMSE estimator. On the other hand, both the Sparse and the Diffuse estimators incur a performance loss, due to their inability to exploit the sparse and the diffuse components jointly, and suffer from poor

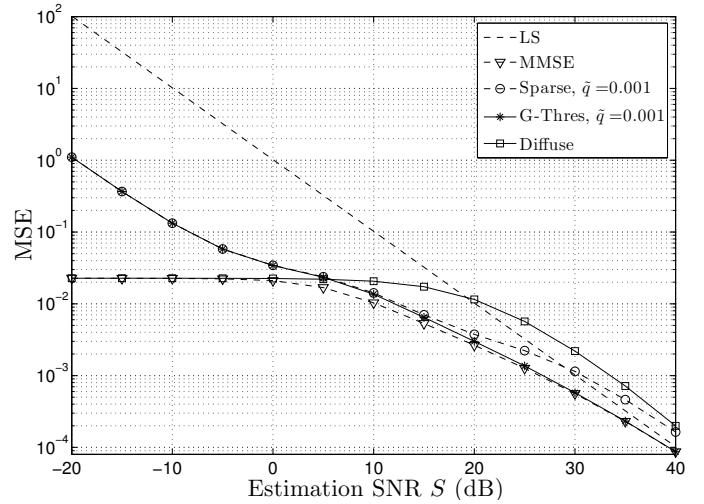


Fig. 3. MSE of the G-Thres, Sparse and Diffuse estimators. The bold lines with the corresponding markers represent the low SNR asymptotic MSE behavior. The high SNR asymptotic behavior is given by the LS estimate.

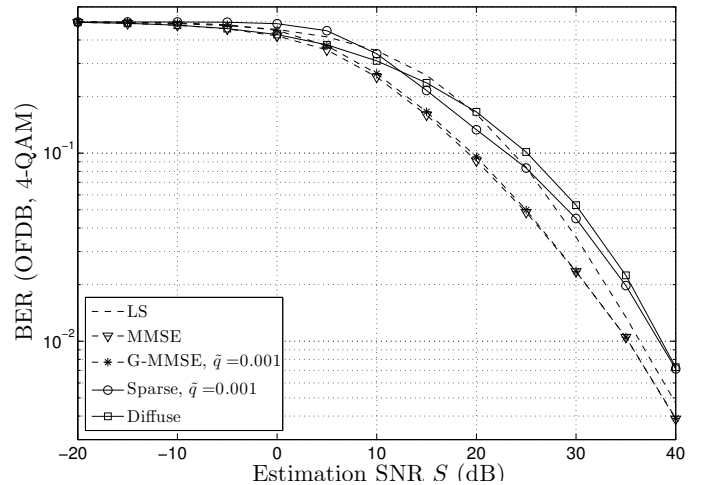


Fig. 4. BER of the G-MMSE, Sparse and Diffuse estimators.

performance for medium and high SNR, attaining a larger BER than LS. This result is in line with the behavior observed in the MSE case.

Finally, in Figure 5 we present the results (mean squared prediction error of the observed sequence) of the evaluation of the proposed estimation strategies based on the SPACE08 experimental data set. The channel is estimated from a single snapshot. In particular, the exponential PDP $\mathcal{P}_d(\cdot)$ (which is unknown *a priori*) is estimated using the Expectation-Maximization algorithm designed in our related work [12]. Despite the fact that the experimental data do not obey the HSD model exactly, we observe that the G-MMSE estimator (with $\tilde{q} = 0.001$) outperforms both the unstructured LS estimator, and the purely Sparse estimator. We refer the interested reader to [16] for further details on the experimental setup and on the results.

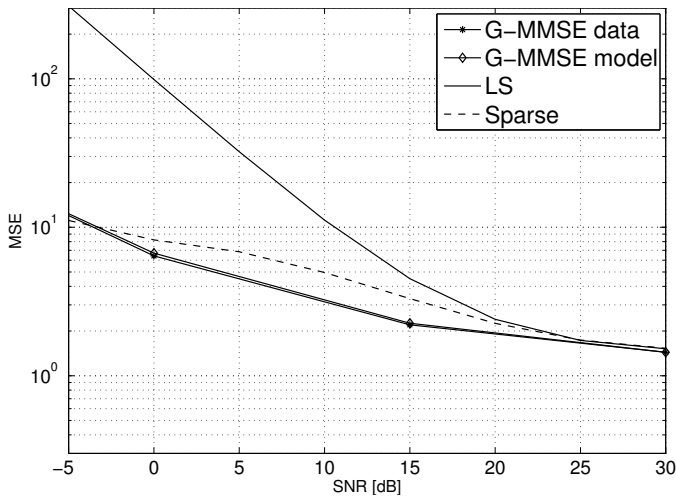


Fig. 5. Mean squared prediction error of the observed sequence from the SPACE08 experimental data set, G-MMSE estimator.

VIII. CONCLUSIONS

In this paper, following [11], we have proposed a novel Hybrid Sparse/Diffuse (HSD) model for the UWA channel, which employs a *sparse component* to model the resolvable MPCs, arising from scattering phenomena and reflections in the environment, and a *diffuse component* to model further propagation phenomena, *e.g.*, unresolvable MPCs, scattering from rough surfaces, frequency dispersion. Based on the analysis of the spatio-temporal evolution of the UWA channel, we have identified four different scenarios, which differ in the amount of side information available at the receiver. Hence, we have proposed estimators based on the HSD model.

Of particular interest are the G-MMSE and the G-Thres estimators, which have been designed for the scenario where the sparse coefficients are treated as deterministic unknown parameters, and the PDP of the diffuse component is known at the receiver. This is relevant when the observation interval is large enough to allow averaging over the small scale fading, but not over the large scale fading. We have developed a MSE analysis of these estimators, showing that a conservative approach in the estimation of the sparse component is beneficial from a MSE perspective, in the high and low SNR regions.

Finally, we have presented simulation results, based on the HSD model, and an evaluation of the proposed techniques based on the SPACE08 experimental data set, which is presented in detail in our previous work [16]. These results show that estimators based on the HSD model considerably improve the MSE and the BER performance over the conventional unstructured Least Squares estimator, and over Sparse and Diffuse estimators, which neglect either the diffuse or the sparse component of the channel. Moreover, we have shown a perfect match between the MSE analysis and the simulation results, which confirms our conjecture that a conservative approach in the estimation of the sparse component is often beneficial, from both a MSE and a BER perspective.

ACKNOWLEDGMENTS

This work has been funded in part by the following grants and organizations: ONR N00014-09-1-0700, NSF CNS-0832186, NSF CNS-0821750 (MRI), Aldo Gini Foundation (Padova, Italy), ONR N00014-10-10422, by the European Commission under the 7th Framework Program (Grant Agreement 258359-CLAM), and by the Italian Institute of Technology within the project SEED framework (NAUTILUS).

The authors would like to thank Beatrice Tomasi and Prof. James C. Preisig for their help and support in the experimental evaluation, based on the SPACE08 data set.

REFERENCES

- [1] I. F. Akyildiz, D. Pompili, and T. Melodia, "State-of-the-art in protocol research for underwater acoustic sensor networks," in *Proceedings of the 1st ACM international workshop on Underwater networks*, New York, NY, USA, 2006, pp. 7–16.
- [2] J. Heidemann, W. Ye, J. Wills, A. Syed, and Y. Li, "Research challenges and applications for underwater sensor networking," in *IEEE Wireless Communications and Networking Conference*, vol. 1, Apr. 2006, pp. 228–235.
- [3] T. Eggen, A. Baggeroer, and J. Preisig, "Communication over Doppler spread channels. Part I: Channel and receiver presentation," *IEEE Journal of Oceanic Engineering*, vol. 25, no. 1, pp. 62–71, Jan. 2000.
- [4] T. Eggen, J. Preisig, and A. Baggeroer, "Communication over Doppler spread channels. Part II: Receiver characterization and practical results," *IEEE Journal of Oceanic Engineering*, vol. 26, no. 4, pp. 612–621, Oct. 2001.
- [5] C. Berger, S. Zhou, J. Preisig, and P. Willett, "Sparse channel estimation for multicarrier underwater acoustic communication: From subspace methods to compressed sensing," *IEEE Transactions on Signal Processing*, vol. 58, no. 3, pp. 1708–1721, Mar. 2010.
- [6] C. Carbonelli, S. Vedantam, and U. Mitra, "Sparse Channel Estimation with Zero Tap Detection," *IEEE Transactions on Wireless Communications*, vol. 6, no. 5, pp. 1743–1763, May 2007.
- [7] A. S. Gupta and J. Preisig, "An adaptive sparse sensing approach to shallow water acoustic channel estimation and tracking," *The Journal of the Acoustical Society of America*, vol. 128, no. 4, pp. 2354–2354, 2010.
- [8] N. Richard and U. Mitra, "Sparse channel estimation for cooperative underwater communications: A structured multichannel approach," in *IEEE International Conference on Acoustics, Speech and Signal Processing (ICASSP)*, Apr. 2008, pp. 5300–5303.
- [9] C. Pelekanakis and M. Chitre, "Comparison of sparse adaptive filters for underwater acoustic channel equalization/estimation," in *International Conference on Communication Systems (ICCS)*, Nov. 2010, pp. 395–399.
- [10] P. Van Walree, "Channel sounding for acoustic communications: techniques and shallow-water examples," Norwegian Defence Research Establishment (FFI), Tech. Rep. FFI-rapport 2011/00007, Apr. 2011. [Online]. Available: rapporter.ffi.no/rapporter/2011/00007.pdf
- [11] N. Michelusi, U. Mitra, and M. Zorzi, "Hybrid Sparse/Diffuse UWB channel estimation," in *International Workshop on Signal Processing Advances in Wireless Communications (SPAWC)*, San Francisco, USA, June 2011, pp. 421–425.
- [12] N. Michelusi, U. Mitra, A. Molisch, and M. Zorzi, "UWB Sparse/Diffuse Channels, Part I: Channel Models and Bayesian Estimators," 2011, submitted to *IEEE Transactions on Signal Processing*.
- [13] —, "UWB Sparse/Diffuse Channels, Part II: Estimator Analysis and Practical Channels," 2011, submitted to *IEEE Transactions on Signal Processing*.
- [14] T. Blumensath and M. Davies, "Iterative Thresholding for Sparse Approximations," *Journal of Fourier Analysis and Applications*, vol. 14, pp. 629–654, 2008, 10.1007/s00041-008-9035-z.
- [15] R. Tibshirani, "Regression shrinkage and selection via the lasso," *Journal of the Royal Statistical Society. Series B (Methodological)*, vol. 58, no. 1, pp. 267–288, 1996.
- [16] N. Michelusi, B. Tomasi, U. Mitra, J. Preisig, and M. Zorzi, "An evaluation of the hybrid sparse/diffuse algorithm for underwater acoustic channel estimation," in *OCEANS 2011*, Sep. 2011.